On the Enhanced Impact Ionization in Uniaxial Strained p-MOSFETs

Pin Su, *Member, IEEE*, and Jack J.-Y. Kuo

***Abstract*—This letter reports a new mechanism for the enhanced impact-ionization rate ($I_{\rm sub}/I_d$) present in short-channel uniaxial strained p-MOSFETs. Through the pinch-off voltage ($V_{\rm dsat}$), we have assessed the impact of strain on the maximum channel electric field. Due to the strain-enhanced mobility, $V_{\rm dsat}$ becomes lower, resulting in the observed V_g-dependent enhancement in $I_{\rm sub}/I_d$. This mechanism needs to be considered when one-to-one comparisons of the hot-carrier effect between strained and unstrained devices are made.**

***Index Terms*—Hot-carrier effect, impact ionization, strained-silicon, substrate current.**

I. Introduction

As STRAINED-silicon is widely used in state-of-the-art CMOS technologies [1]–[4] to enable the mobility scaling [5], the hot-carrier effect is another important scaling issue that has to be considered for strained MOSFETs.

II. Results and Discussion

The hot-carrier effect is usually monitored by the substrate current ($I_{\rm sub}$) [6]. $I_{\rm sub}$ results from the impact ionization caused by energetic carriers in the channel. Several authors [7]–[9] have reported the strain-induced enhancement of impact-ionization rate ($I_{\rm sub}/I_d$). Irisawa *et al.* [7] examined long-channel strained MOSFETs and attributed the enhanced $I_{\rm sub}/I_d$ to the reduced bandgap energy. Whether there is any other physical mechanism responsible for the strain-enhanced impact ionization merits further examination.

$I_{\rm sub}$ has long been closely related to the maximum channel electric field (E_m) near the drain [6]. With the strain-induced enhancement of carrier mobility, E_m may vary and may play a crucial role in one-to-one comparisons of the hot-carrier effect between strained and unstrained devices. In this letter, we investigate the substrate current in short-channel uniaxial strained p-MOSFETs and report a new mechanism responsible for the strain-enhanced impact ionization.

Manuscript received March 26, 2007; revised May 4, 2007. This work was supported in part by the National Science Council of Taiwan, R.O.C., under Contract NSC95-2221-E-009-327-MY2 and in part by the MoE ATU Program 95W803. The review of this letter was arranged by Editor K. De Meyer.

The authors are with the Department of Electronics Engineering, National Chiao Tung University, Hsinchu 300, Taiwan, R.O.C. (e-mail: pinsu@mail.nctu.edu.tw).

Color versions of one or more of the figures in this letter are available online at http://ieeexplore.ieee.org.

Digital Object Identifier 10.1109/LED.2007.900297

Co-processed strained and unstrained p-MOSFETs are investigated in this study. The strained devices were fabricated by state-of-the-art process-induced uniaxial strained-silicon technology featuring SiGe source/drain and compressive contact etch stop layer (CESL) [10]. For the transistors with gate length $L_{\rm gate} = 65$ nm, the saturation drain current (I_d) of the strained device is improved more than 85% as compared with its control counterpart.

Fig. 1(a) shows the gate-bias dependence of the measured $I_{\rm sub}$ for the strained and control devices. Typical bell-shape characteristics can be seen. Fig. 1(b) shows that the impact-ionization rate of the strained device is larger than that of the unstrained one. The strain-induced enhancement in $I_{\rm sub}/I_d$ increases with gate bias.

According to the lucky electron model [11]

$$\frac{I_{\rm sub}}{I_d} \propto e^{-\frac{\varphi_i}{q\lambda E_m}} \tag{1}$$

where φ_i is the energy required for impact ionization, and λ is the mean-free path. Although the strain-induced reduction in bandgap energy (hence, φ_i) may raise the impact-ionization rate for the strained device [7], it cannot explain the gate-bias dependence of the enhancement in $I_{\rm sub}/I_d$ as observed in Fig. 1(b).

The V_g dependence of $I_{\rm sub}/I_d$ stems from E_m, the maximum channel electric field. E_m can be modeled [6] as

$$E_m = \frac{V_d - V_{\rm dsat}}{l} \tag{2}$$

where $V_{\rm dsat}$ is the potential at the pinch-off (i.e., saturation) point in the channel, and l is the characteristic length in the pinch-off region. Although E_m cannot be directly measured, the impact of strain on E_m can be assessed through $V_{\rm dsat}$. From the output resistance ($R_{\rm out}$) versus V_d plot (Fig. 2), $V_{\rm dsat}$ can be extracted by linear extrapolation because $R_{\rm out}$ is proportional to $V_d - V_{\rm dsat}$ in the channel-length modulation region [12], [13]. It can be seen from Fig. 2 that the strained device has a smaller $V_{\rm dsat}$ than its control counterpart for a given gate voltage overdrive ($V_{\rm gst}$).

Fig. 3 shows the $V_{\rm gst}$ dependence of the extracted $V_{\rm dsat}$. The strain-induced reduction (i.e., the discrepancy between the control and strained devices) in $V_{\rm dsat}$ increases with gate bias. It explains why in Fig. 1(b) the strain-induced enhancement in $I_{\rm sub}/I_d$ increases with gate bias.

The strain-reduced $V_{\rm dsat}$ results from the enhanced mobility in the strained device. The enhancement in mobility

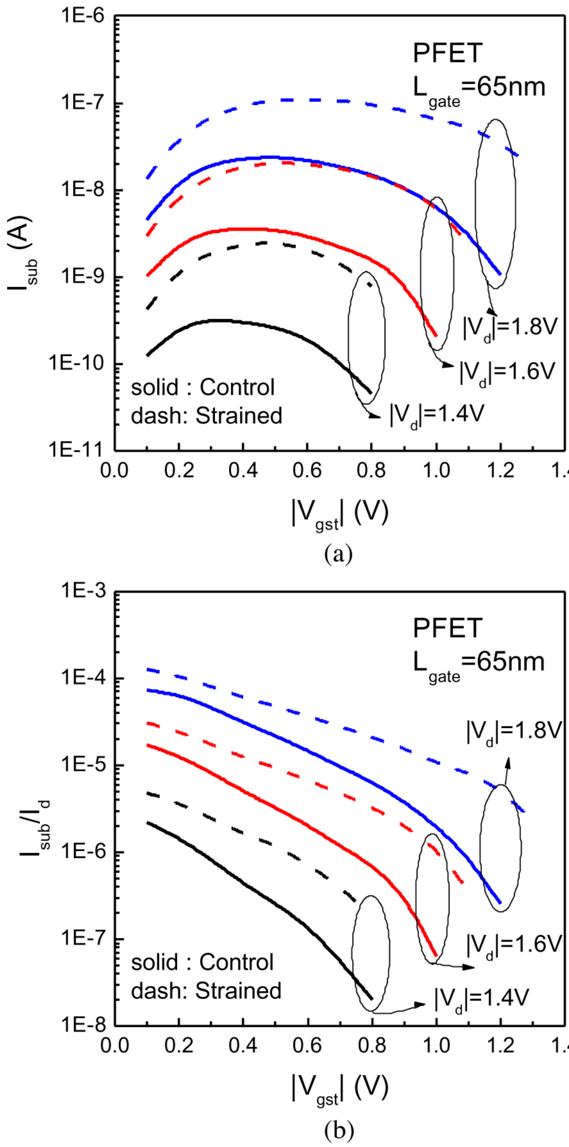

Fig. 1. (a) I_{sub} versus gate voltage overdrive (V_{gst}) for the strained and control devices with various drain biases. (b) I_{sub}/I_d versus V_{gst} showing the strain-enhanced impact ionization.

corresponds to an increase in slope of the carrier velocity versus lateral field characteristic [14] and a reduction in the critical field (E_{sat}) for velocity saturation [15], [16]. Since V_{dsat} is essentially determined by E_{sat} in the high V_{gst} regime [6], [16], the impact of strain on V_{dsat}, as shown in Fig. 3, becomes significant with increasing gate bias.

The strain-reduced V_{dsat} enhances the impact-ionization rate and needs to be considered in monitoring the hot-carrier effect of the strained device. Fig. 4 shows that, with the extracted V_{dsat} from Fig. 3, the same I_{sub} data (Fig. 1) reduce to a single straight line for the control and strained devices, respectively, when $\ln(I_{\mathrm{sub}}/I_d)$ is plotted against $1/(V_d - V_{\mathrm{dsat}})$ as predicted by (1) and (2). In Fig. 4, the slope of the strained device is about 9.5% smaller than that of the unstrained device. Since the slope is proportional to $\varphi_i l/\lambda$, we can estimate from Fig. 4 that the upper bound of the bandgap change due to strain is 9.5%. The reduced slope for the strained device has also been reported by Irisawa *et al.* [7], who attributed it mainly to the reduced bandgap energy. Our expected value of the bandgap change is between 5% to 10%.

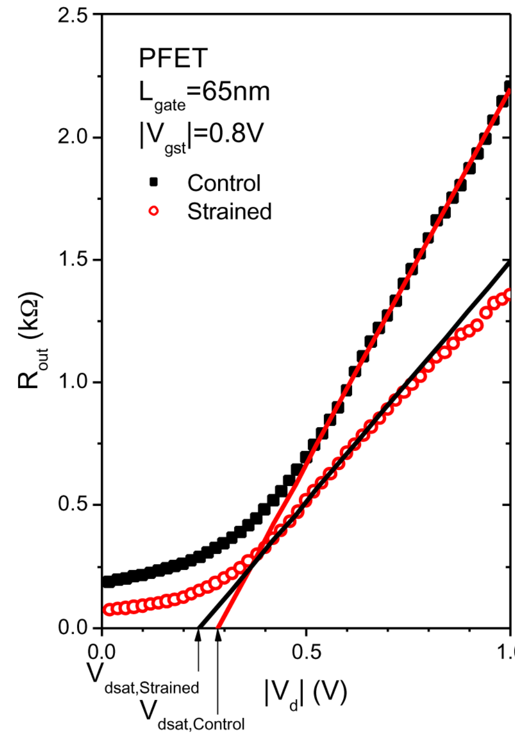

Fig. 2. R_{out} versus V_d plot can be used to determine V_{dsat}. The strained device has a smaller V_{dsat} than its control counterpart for a given V_{gst}.

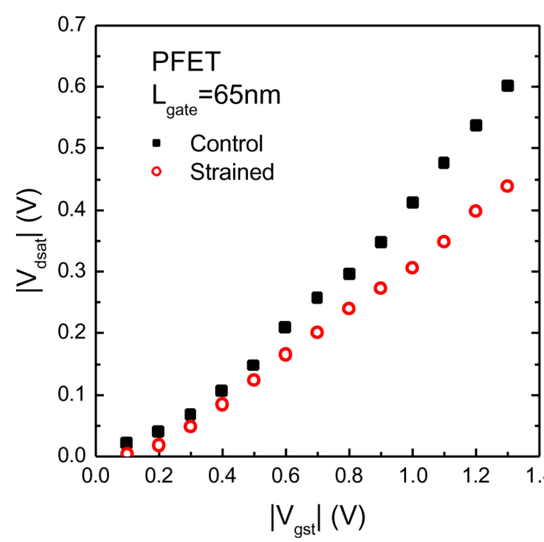

Fig. 3. Impact of strain on V_{dsat} increases with V_{gst}.

III. Conclusion

In conclusion, we report a new mechanism for the enhanced impact ionization present in short-channel uniaxial strained p-MOSFETs. Due to the strain-enhanced mobility, V_{dsat} becomes lower, resulting in the observed V_g-dependent enhancement in I_{sub}/I_d. This mechanism is important and needs to be considered when one-to-one comparisons of the hot-carrier effect between strained and unstrained devices are made.

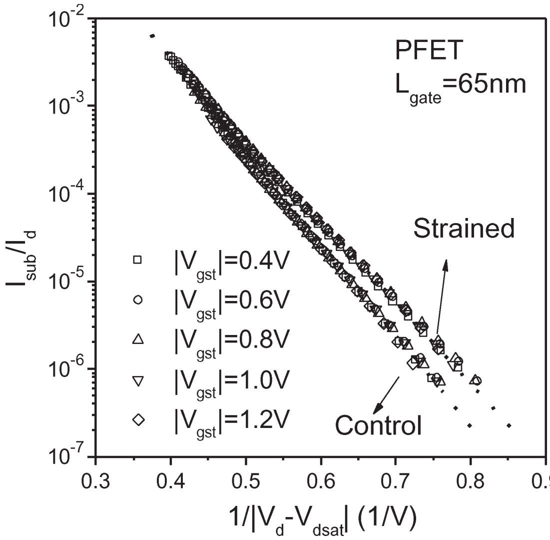

Fig. 4. Strained-reduced V_{dsat} needs to be considered in the construction of the $\ln(I_{\mathrm{sub}}/I_d)$ versus $1/(V_d - V_{\mathrm{dsat}})$ plot for monitoring the hot-carrier effect of the strained device.

ACKNOWLEDGMENT

The authors would like to thank W. P.-N. Chen for the help during the work.

REFERENCES

[1] S. Tyagi, C. Auth, P. Bai, G. Curello, H. Deshpande, S. Gannavaram, O. Golonzka, R. Heussner, R. James, C. Kenyon, S.H. Lee, N. Lindert, M. Liu, R. Nagisetty, S. Natarajan, C. Parker, J. Sebastian, B. Sell, S. Sivakumar, A. St Amour, and K. Tone, “An advanced low power, high performance, strained channel 65 nm technology,” in *IEDM Tech. Dig.*, 2005, pp. 245–248.

[2] S. E. Thompson, G. Sun, Y. S. Choi, and T. Nishida, “Uniaxial-process-induced strained-Si: Extending the CMOS roadmap,” *IEEE Trans. Electron Devices*, vol. 53, no. 5, pp. 1010–1020, May 2006.

[3] E. X. Wang, P. Matagne, L. Shifren, B. Obradovic, R. Kotlyar, S. Cea, M. Sterrler, and M. D. Giles, “Physics of hole transport in strained silicon MOSFET inversion layers,” *IEEE Trans. Electron Devices*, vol. 53, no. 8, pp. 1840–1843, Aug. 2006.

[4] X. Chen, S. Fang, W. Gao, T. Dyer, Y. W. Teh, S. S. Tan, Y. Ko, C. Baiocco, A. Ajmera, J. Park, J. Kim, R. Stierstorfer, D. Chidambarrao, Z. Luo, N. Nivo, P. Nguyen, J. Yuan, S. Panda, O. Kwon, N. Edleman, T. Tjoa, J. Widodo, M. Belyansky, M. Sherony, R. Amos, H. Ng, and M. Hierlemann, “Stress proximity technique for performance improvement with dual stress linear at 45 nm technology and beyond,” in *VLSI Symp. Tech. Dig.*, 2006, pp. 60–61.

[5] C. Hu, “Device challenges and opportunities,” in *VLSI Symp. Tech. Dig.*, 2004, p. 4.

[6] C. Hu, S. C. Tam, F. C. Hsu, P. K. Ko, T. Y. Chan, and K. W. Terrill, “Hot-electron-induced MOSFET degradation—Model, monitor, and improvement,” *IEEE Trans. Electron Devices*, vol. ED-32, no. 8, pp. 375–385, Aug. 1985.

[7] T. Irisawa, T. Numata, N. Sugiyama, and S. Takagi, “On the origin of increase in substrate and impact ionization efficiency in strained-Si n- and p-MOSFETs,” *IEEE Trans. Electron Devices*, vol. 52, no. 5, pp. 993–998, May 2005.

[8] N. Watanabe, T. Kojima, Y. Maeda, M. Nishisaka, and T. Asano, “Breakdown voltage in uniaxially strained n-channel SOI MOSFET,” *Jpn. J. Appl. Phys.*, vol. 43, no. 4B, pp. 2134–2139, Apr. 2004.

[9] S. S. Chung, D. C. Huang, Y. J. Tsai, C. S. Lai, C. H. Tsai, P. W. Liu, Y. H. Lin, C. T. Tsai, G. H. Ma, S. C. Chien, and S. W. Sun, “New observation on the uniaxial and biaxial strain-induced hot carrier and NBTI reliabilities for 65 nm node CMOS devices and beyond,” in *IEDM Tech. Dig.*, 2006, pp. 1–4.

[10] J. Kuo, W. Chen, and P. Su, “Investigation of analog performance for process-induced-strained pMOSFETs,” *Semicond. Sci. Technol.*, vol. 22, no. 4, pp. 404–407, Apr. 2007.

[11] Y. A. El Mansy and D. M. Caughey, “Modeling weak avalanche multiplication currents in IGFETs and SOS transistors for CAD,” in *IEDM Tech. Dig.*, 1975, p. 31.

[12] J. H. Huang, Z. H. Liu, M. C. Jeng, P. K. Ko, and C. Hu, “A physical model for MOSFET output resistance,” in *IEDM Tech. Dig.*, 1992, pp. 569–572.

[13] Y. Cheng and C. Hu, *MOSFET Modeling & BSIM3 User’s Guide*. Norwell, MA: Kluwer, 1999. KAP.

[14] M. Saitoh and K. Uchida, “Universal relationship between low-field mobility and high-field carrier velocity in high-κ and SiO_2 gate dielectric MOSFETs,” in *IEDM Tech. Dig.*, 2006, pp. 261–264.

[15] C. Sodini, P. Ko, and J. Moll, “The effect of high fields on MOS device and circuit performance,” *IEEE Trans. Electron Devices*, vol. ED-31, no. 10, p. 1386, Oct. 1984.

[16] Y. Taur and T. H. Ning, *Fundamentals of Modern VLSI Devices*. Cambridge, U.K.: Cambridge Univ. Press, 1998, p. 150.